

Low-frequency noise of intrinsic gated region in AlN/AlGaIn/GaN metal-insulator-semiconductor heterojunction field-effect transistors

S. P. Le, T. Q. Nguyen, H.-A. Shih, M. Kudo, and T. Suzuki*

Center for Nano Materials and Technology, Japan Advanced Institute of Science and Technology (JAIST)

1-1 Asahidai, Nomi, Ishikawa 923-1292, Japan *E-mail: tosikazu@jaist.ac.jp, Phone: +81-761-51-1441

1 Introduction

GaN-based metal-insulator-semiconductor heterojunction field-effect transistors (MIS-HFETs) have been extensively developed owing to the merits of gate leakage reduction and passivation effects. As a gate insulator, high-dielectric-constant (high- k) oxides, such as Al_2O_3 [1] or HfO_2 [2], and also high- k nitrides having merits of high thermal conductivities, such as AlN [3, 4] or BN [5, 6], were employed. In the GaN-based MIS-HFETs, low-frequency noise (LFN) will be strongly influenced by the insulator itself and/or the insulator-semiconductor interface, and also by the gate leakage reduction. Although LFN in the GaN-based devices has been studied for a long time, the previous studies mainly focused on Schottky-HFETs [7–9] and MIS-HFETs with the oxide gate insulators [10]. Moreover, in many previous studies, it is difficult to identify the contribution from the intrinsic gated region and extrinsic ungated region. Therefore, it is important to obtain insights of LFN in GaN-based MIS-HFETs with nitride insulators, clarifying the contribution from the intrinsic and extrinsic regions. In this work, we systematically investigated LFN characteristics in AlN/AlGaIn/GaN MIS-HFETs with the AlN insulator deposited by RF sputtering on the AlGaIn. In combination with investigation of LFN in AlN/AlGaIn/GaN ungated two-terminal devices, we extracted LFN behaviors of the intrinsic gated region in the MIS-HFETs.

2 Device fabrication and characterization

Using $\text{Al}_{0.3}\text{Ga}_{0.7}\text{N}(30\text{ nm})/\text{GaN}(3000\text{ nm})$ heterostructure obtained by metal-organic vapor phase epitaxy on sapphire(0001), we fabricated AlN/AlGaIn/GaN MIS-HFETs as well as AlN/AlGaIn/GaN ungated two-terminal devices. The fabrication process is as follows. On the heterostructure, Ti/Al/Ti/Au Ohmic electrodes were formed and device isolation was achieved by B⁺ implantation. A 20 nm AlN film as the insulator layer was deposited on the AlGaIn surface by RF magnetron sputtering at room temperature with an AlN target in Ar-N₂ ambient, completing the ungated two-terminal devices. For the MIS-HFETs, finally Ni/Au gate electrodes were formed. From transfer length method (TLM) measurements of the ungated devices with electrode spacing $L = 2\text{--}16\ \mu\text{m}$ and width $W = 50, 100\ \mu\text{m}$, we obtain a sheet resistance of $800\ \Omega/\text{sq.}$ and a contact resistance of $2.4\ \Omega\text{mm}$. The MIS-HFETs with gate length $L_G = 260\text{ nm}$, width $W = 50\ \mu\text{m}$, source-gate spacing $2\ \mu\text{m}$, and gate-drain spacing $3\ \mu\text{m}$ exhibit output and transfer characteristics shown in Fig. 1.

We firstly investigated LFN in the ungated devices. As shown in Figs. 2 (a) and (b), we observed current noise power spectrum density $S_I \simeq KI^2/f$, with the current I , the frequency f , and a constant factor K . We obtain

the relation between the KW and RW , where R is the total resistance, shown in Fig. 2(c). A Hooge parameter of the ungated region $\alpha_{\text{ug}} \simeq 2 \times 10^{-4}$ is estimated from the size dependence of K . LFN in the MIS-HFETs for the linear regime of drain-source voltage V_D was obtained with changing gate-source voltage V_G as shown in Figs. 3 (a) and (b), exhibiting $S_{I_D} \simeq K_{\text{HFET}} I_D^2/f$, with the drain current I_D and a constant factor K_{HFET} . Since the total on-resistance R_{on} is the sum of the intrinsic resistance $R_{\text{int}} = rL_G/W$, where r is the sheet resistance of the gated region, and the extrinsic resistance R_{ext} of the ungated part, we obtain

$$K_{\text{HFET}} = K_{\text{int}} \frac{R_{\text{int}}^2}{R_{\text{on}}^2} + K_{\text{ext}} \frac{R_{\text{ext}}^2}{R_{\text{on}}^2}, \quad (1)$$

with the factor K_{int} from the intrinsic gated region and K_{ext} from the extrinsic ungated part; the latter is estimated to be $K_{\text{ext}} \simeq 4 \times 10^{-11}$ from the relation shown in Fig. 2(c). Thus, from (1), we obtain K_{int} as a function of r as shown in Fig. 4(a); with increase in r , we observe behavior changing from $K_{\text{int}} \propto r^{-2}$ to $\propto r^2$. Using the under-gate sheet electron concentration n_s obtained by C - V measurements, we can calculate the effective Hooge parameter of the intrinsic gated region $\alpha = K_{\text{int}}N$, where $N = n_sL_GW$ is the number of electrons under the gate. Figure 4(b) shows α as a function of n_s , with the point of α_{ug} for the ungated region. For the small $n_s \lesssim 5 \times 10^{11}\text{ cm}^{-2}$, with increase in n_s , we obtain decrease in $\alpha \propto n_s^{-1}$. This behavior is also observed for the Schottky-HFETs [8, 9], and can be attributed to the electron number fluctuation due to traps near the AlGaIn/GaN interface. On the other hand, for $5 \times 10^{11}\text{ cm}^{-2} \lesssim n_s \lesssim 1 \times 10^{12}\text{ cm}^{-2}$, α decreases rapidly like $n_s^{-\xi}$ with $\xi \sim 2\text{--}3$, which is not observed for the Schottky-HFETs. We tentatively assume that this behavior is attributed to the mobility fluctuation specific for the MIS-HFETs. Moreover, we obtain strong increase in $\alpha \propto n_s^3$ for $n_s \gtrsim 2 \times 10^{12}\text{ cm}^{-2}$. Strong increase in α for large V_G and n_s is also observed in the Schottky-HFETs, sometimes being attributed to large gate leakage currents [9]. However, in the MIS-HFETs, this behavior cannot be attributed to the gate leakage, which is significantly suppressed, but can be related to the fluctuation in the intrinsic gate voltage, which is enhanced for large V_G and n_s by the fluctuation of the voltage across the extrinsic source resistance. According to this, α of the gated region is larger than α_{ug} of the ungated region for the same sheet electron concentration, as confirmed in the Fig. 4(b). Even for the intrinsic gated region, the LFN can be influenced by the extrinsic part through the fluctuation of the intrinsic gate voltage.

3 Summary

We systematically investigated LFN in the AlN/AlGaIn/GaN MIS-HFETs. In combination with investigation of LFN in the ungated devices, we obtained the LFN behavior of the intrinsic gated region in the MIS-HFETs.

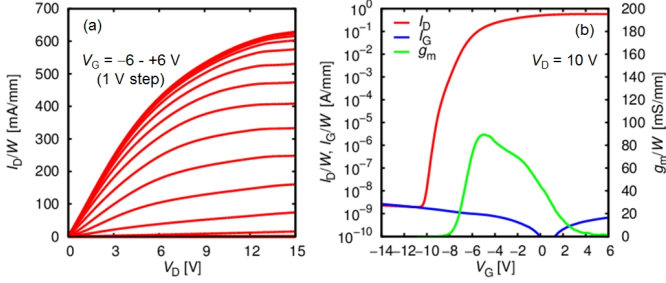


Fig. 1: (a) Output and (b) transfer characteristics of the AlN/AlGaIn/GaN MIS-HFET. Drain current I_D , gate current I_G , and transconductance g_m , all normalized by the gate width W , are shown.

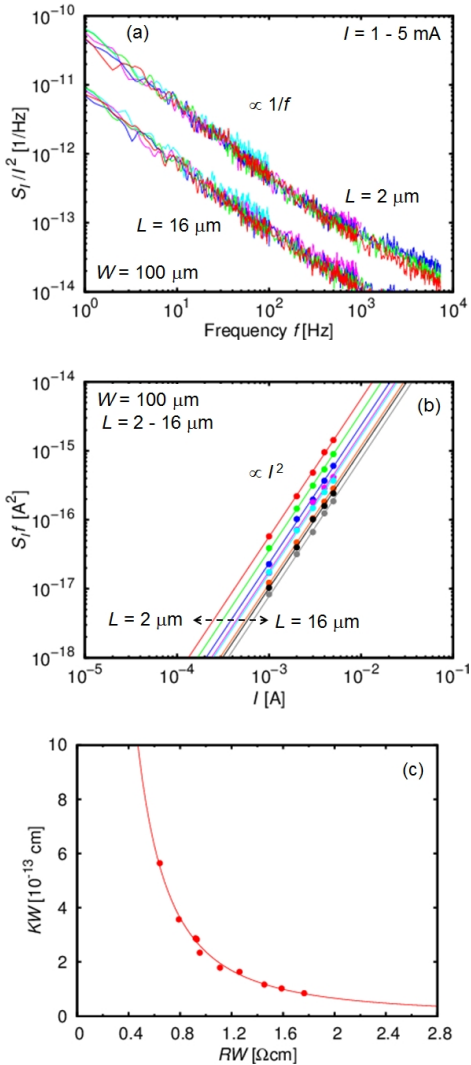


Fig. 2: (a) S_I/I^2 as a function of f and (b) $S_I f$ as a function of I for the ungated devices. (c) The relation between KW and RW for the ungated devices.

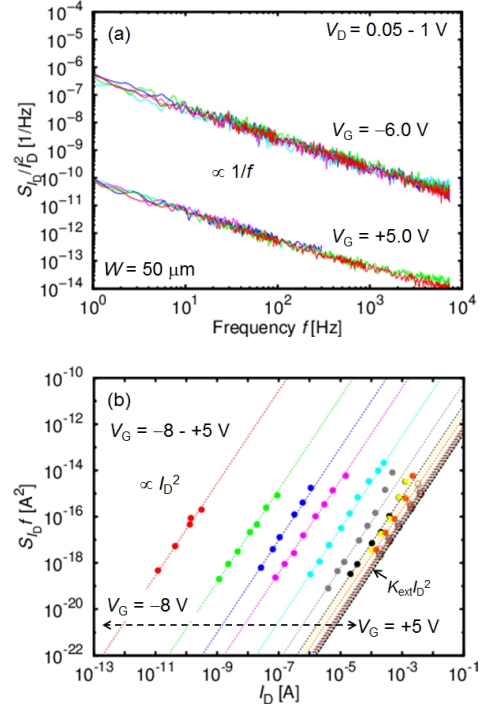


Fig. 3: (a) S_{I_D}/I_D^2 as a function of f and (b) $S_{I_D} f$ as a function of I_D for the MIS-HFETs.

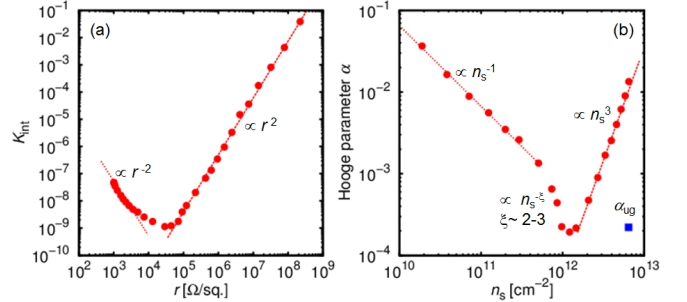


Fig. 4: (a) K_{int} as a function of r and (b) α as a function of n_s for the gated region, with the point of α_{ug} for the ungated region.

References

- [1] T. Hashizume, S. Ootomo, and H. Hasegawa, Appl. Phys. Lett. **83**, 2952 (2003).
- [2] C. Liu, E. F. Chor, and L. S. Tan, Appl. Phys. Lett. **88**, 173504 (2006).
- [3] Y. Liu, J. A. Bardwell, S. P. McAlister, S. Rolfe, H. Tang, and J. B. Webb, Phys. Status Solidi C **0**, 69 (2002).
- [4] H.-A. Shih, M. Kudo, and T. Suzuki, Appl. Phys. Lett. **101**, 043501 (2012).
- [5] J.-C. Gerberdoen, A. Soltani, M. Mattalah, M. Moreau, P. Thevenin, and J.-C. D. Jaeger, Diam. Relat. Mater. **18**, 1039 (2009).
- [6] T. Q. Nguyen, H.-A. Shih, M. Kudo, and T. Suzuki, Phys. Status Solidi C **10**, 1401 (2013).
- [7] M. E. Levinshtein, F. Pascal, S. Contreras, W. Knap, S. L. Rumyantsev, R. Gaska, J. W. Yang, and M. S. Shur, Appl. Phys. Lett. **72**, 3053 (1998).
- [8] J. A. Garrido, B. E. Foutz, J. A. Smart, J. R. Shealy, M. J. Murphy, W. J. Schaff, L. F. Eastman, and E. Muoz, Appl. Phys. Lett. **76**, 3442 (2000).
- [9] N. Pala, S. Rumyantsev, M. Shur, R. Gaska, X. Hu, J. Yang, G. Simin, and M. Khan, Solid-State Electron. **47**, 1099 (2003).
- [10] C. Kayis, J. H. Leach, C. Zhu, M. Wu, X. Li, U. Özgür, H. Morkoc, X. Yang, V. Misra, and P. Handel, IEEE Electron Device Lett. **31**, 1041 (2010).